The A-type domain in *Escherichia coli* NfuA is required for regenerating the auxiliary [4Fe–4S] cluster in *Escherichia coli* lipoyl synthase

Received for publication, October 9, 2018, and in revised form, December 10, 2018 Published, Papers in Press, December 11, 2018, DOI 10.1074/jbc.RA118.006171

Erin L. McCarthy[‡], **Ananda N. Rankin**[§], **Zerick R. Dill**[§], **and Squire J. Booker**[‡§¶1]

From the [‡]*Department of Biochemistry and Molecular Biology, The Pennsylvania State University, University Park, Pennsylvania 16802,* [§]*Department of Chemistry, The Pennsylvania State University, University Park, Pennsylvania 16802, and* [¶]*Howard Hughes Medical Institute, The Pennsylvania State University, University Park, Pennsylvania 16802*

Edited by Joseph M. Jez

The lipoyl cofactor plays an integral role in several essential biological processes. The last step in its *de novo* biosynthetic pathway, the attachment of two sulfur atoms at C6 and C8 of an *n*-octanoyllysyl chain, is catalyzed by lipoyl synthase (LipA), a member of the radical SAM superfamily. In addition to the [4Fe–4S] cluster common to all radical SAM enzymes, LipA contains a second [4Fe–4S] auxiliary cluster, which is sacrificed during catalysis to supply the requisite sulfur atoms, rendering the protein inactive for further turnovers. Recently, it was shown that the Fe–S cluster carrier protein NfuA from *Escherichia coli* can regenerate the auxiliary cluster of *E. coli* LipA after each turnover, but the molecular mechanism is incompletely understood. Herein, using protein–protein interaction and kinetic assays as well as site-directed mutagenesis, we provide further insight into the mechanism of NfuA-mediated cluster regeneration. In particular, we show that the N-terminal A-type domain of *E. coli* NfuA is essential for its tight interaction with LipA. Further, we demonstrate that NfuA from *Mycobacterium tuberculosis* can also regenerate the auxiliary cluster of *E. coli* LipA. However, an Nfu protein from *Staphylococcus aureus*, which lacks the A-type domain, was severely diminished in facilitating cluster regeneration. Of note, addition of the N-terminal domain of *E. coli* NfuA to *S. aureus* Nfu, fully restored cluster-regenerating activity. These results expand our understanding of the newly discovered mechanism by which the auxiliary cluster of LipA is restored after each turnover.

Since its initial identification by Sofia *et al.* in 2001, the radical SAM (RS)[2] superfamily has expanded to include almost 114,000 individual sequences representing more than 85 distinct reactions (1, 2). Members of the RS superfamily coordinate a [4Fe–4S] which, in its reduced state, is used to fragment *S*-adenosylmethionine (SAM) to methionine and a 5′-deoxyadenosin 5′-radical (5′-dA•) (3). Lipoyl synthase (LipA) uses the 5′-dA• intermediate to catalyze the last step of the *de novo* pathway for the biosynthesis of the lipoyl cofactor, which is the attachment of sulfur atoms at C6 and C8 of an *n*-octanoyllysyl chain on a lipoyl carrier protein. LipA belongs to a subclass of RS enzymes that contain additional auxiliary iron–sulfur (Fe–S) clusters, which further diversifies the chemical repertoire of the superfamily (4). The [4Fe–4S] auxiliary cluster of LipA has been shown to be cannibalized by the protein during catalysis to provide the sulfur atoms in the lipoyl product. Although this sacrificial role for an Fe–S cluster has been controversial, given that its destruction inactivates the protein, an abundance of biochemical, spectroscopic, and crystallographic evidence support it (5–10).

All organisms have established and highly regulated pathways for Fe–S cluster assembly which share some basic components (11–13), and it seemed likely that these pathways might be involved in regenerating LipA's auxiliary cluster after each turnover. Briefly, a cysteine desulfurase provides sulfur from cysteine, whereas a still-debated source supplies iron to a general scaffold protein upon which an Fe–S cluster is assembled. In a poorly understood process, the scaffold protein transfers a cluster to targeting proteins, which recognize their targets and transfer newly assembled clusters to them. Defects in Fe–S cluster assembly in humans result in a number of prevalent disorders, such as Friedreich's ataxia and multiple mitochondrial dysfunctions disorder (14).

Recently, *E. coli* NfuA, a previously characterized intermediate Fe–S cluster carrier protein, was shown to restore the auxiliary cluster in LipA after each turnover in a process that does not limit the overall rate of catalysis (15–17). *E. coli* NfuA is composed of two distinct domains: a "degenerate" A-type N-terminal domain and an Nfu-like C-terminal domain, and previous studies have provided evidence for a role for both of these two domains in NfuA's function (18). Because LipA has now been established as a target for NfuA, we can exploit this system to better understand the roles of these two domains in Fe–S protein targeting and Fe–S cluster regeneration.

This work was supported by National Institutes of Health Grant GM-122595 and National Science Foundation Grants MCB-1716686 and CHE-1659679. This work was also supported by the Howard Hughes Medical Institute EXROP program (to Z. R. D.). The authors declare that they have no conflicts of interest with the contents of this article. The content is solely the responsibility of the authors and does not necessarily represent the official views of the National Institutes of Health.

This article contains Figs. S1–S6 and Tables S1 and S2.

[1] A Howard Hughes Medical Institute investigator. To whom correspondence should be addressed: 302 Chemistry Bldg., University Park, PA 16802. Tel.: 814-865-8793; E-mail: squire@psu.edu.

[2] The abbreviations used are: RS, radical SAM; SAM, *S*-adenosylmethionine; LipA, lipoyl synthase; 5′-dA•, 5′-deoxyadenosyl 5′-radical; *Mt, Mycobacterium tuberculosis*.

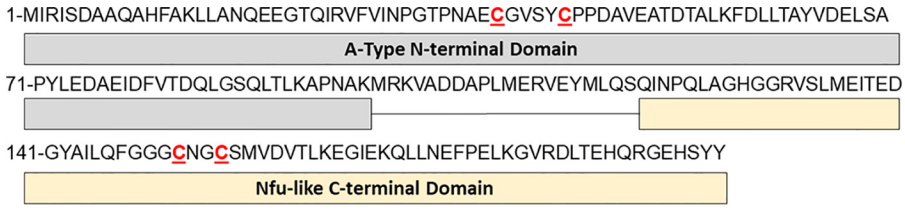

Figure 1. Amino acid sequence and domain architecture of *E. coli* NfuA. NfuA is composed of two distinct domains: An N-terminal A-type domain (*gray*) and a C-terminal Nfu-like domain (*pale yellow*). The sequence contains four cysteinyl residues (*red*): Two in the N-terminal domain and two in the C-terminal domain.

Results

Role of NfuA cysteine residues in cluster coordination and transfer

NfuA contains four cysteine residues, two of which are in its N-terminal A-type domain (Cys-39 and Cys-44), and two of which are in its C-terminal Nfu-like domain (Cys-149 and Cys-152) (Fig. 1). To assess the importance of each of the cysteine residues on NfuA's ability to enhance LipA catalysis, each was individually changed to an alanine residue, yielding four variant proteins. When Cys-39 or Cys-44 is changed to alanine, the resulting variant protein is as capable as WT NfuA of ligating a [4Fe–4S] cluster (Fig. S1*A*) and can enhance LipA turnover, although to a lesser extent (Fig. 2). In the absence of NfuA, 25 μM LipA catalyzes formation of ~20 μM lipoyl product in 2.5 h (Fig. 2, *closed circles*). In the presence of 400 μM (200 μM active dimer) NfuA variant, 25 μM LipA catalyzes formation of 140 μM (C44A) or 120 μM (C39A) lipoyl product in 2.5 h, whereas 170 μM product is formed in the presence of WT NfuA (Fig. 2, *closed triangles*, C39A variant; *closed squares*, C44A variant; *open squares*, WT NfuA), indicating that the variant proteins can restore LipA's auxiliary cluster. By contrast, when Cys-149 or Cys-152 is changed to alanine, the ability of the variant protein to ligate a [4Fe–4S] cluster (Fig. S1*B*) and to enhance LipA turnover (Fig. 2, *blue open circles* and *red open triangles*) is abrogated. In these instances, LipA catalyzes significantly less than one turnover, suggesting that these NfuA variants inhibit LipA turnover. These results confirm the role of the two C-terminal cysteines in [4Fe–4S] cluster coordination and show that that the two N-terminal cysteines do not function in cluster transfer to LipA under the given reaction conditions. An earlier study in which the two N-terminal cysteine residues were substituted with serine residues reported that these variants could still coordinate a cluster (15). However, this observed difference may be because serine residues can participate in cluster coordination, as is the case for the auxiliary cluster of LipA as well as other variants of Fe–S proteins (19, 20).

E. coli NfuA N-terminal domain is essential for tightly interacting with LipA

Currently, there is no well-defined function for the so-called degenerate A-type N-terminal domain of *E. coli* NfuA, although it has been proposed to play a role in protein–protein interactions (18). We investigated the role of the N-terminal domain in regenerating the auxiliary cluster of LipA by isolating and characterizing a fragment of NfuA (N-terminal domain) containing amino acid residues 1–97. This truncated domain has been shown to exhibit a far-UV CD spectrum that is identical to that of the full-length protein (18). We subjected the

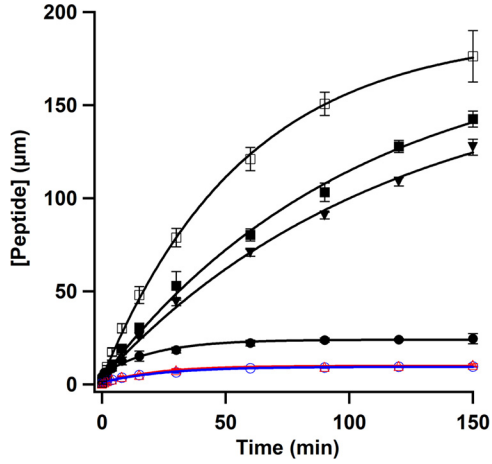

Figure 2. *E. coli* LipA activity in the presence of *E. coli* NfuA WT, C39A, C44A, C149A, and C152A. *A*, effect of NfuA C39A (*closed triangles*), C44A (*closed squares*), C149A (*blue open circles*), and C152A (*red open triangles*) variants on LipA catalysis. LipA only control (*closed circles*). LipA and NfuA control (*open squares*). Reactions were performed at room temperature and included 25 μM LipA, 400 μM NfuA variant or WT protein, 400 μM peptide substrate, 1 mM SAM, and 0.5 μM SAH nucleosidase. Reactions were initiated by the addition of 2 mM dithionite and quenched at various times with H_2SO_4 at a final concentration of 100 mM. *Error bars* represent the mean ± S.D. of three replicates.

NfuA N-terminal domain to UV-visible spectroscopy and analyzed its effect on the activity of LipA. As expected, the UV-visible spectrum of the NfuA N-terminal domain shows no features that are indicative of an Fe–S cluster (Fig. 3). Further, the N-terminal domain does not have any apparent effect on LipA's activity (Fig. 4). In the presence of 400 μM (200 μM active dimer) WT NfuA, 25 μM LipA catalyzes formation of almost 200 μM lipoyl product in 2.5 h (Fig. 4, *closed black squares*). By contrast, in the absence of NfuA (Fig. 4, *closed red circles*), or when full-length NfuA is replaced by its N-terminal domain (Fig. 4, *closed blue circles*), 25 μM LipA catalyzes formation of slightly less than 25 μM product. To determine whether the N-terminal domain of NfuA might be involved in protein–protein interactions, as has been suggested previously (18), its tight association with LipA was assessed by molecular-sieve chromatography (Fig. 5*A* and Fig. S2). LipA alone (*dotted trace*) elutes at 60.6 ml, corresponding to an experimental mass of 44.3 kDa (theoretical mass is 38.2 kDa). The N-terminal domain of NfuA elutes at 75.3 ml (*dashed trace*), corresponding to an experimental mass of 12.5 kDa (theoretical mass is 12.6 kDa). The sample containing an equimolar mixture of LipA and the NfuA N-terminal domain (*solid trace*) elutes at 58.6 ml as a major peak, corresponding to an experimental mass of 52.4 kDa, which suggests a 1:1 complex between the two proteins (theoretical mass is 50.8 kDa). Fractions corresponding to the major peak were subjected to analysis by SDS-PAGE, and two bands corresponding

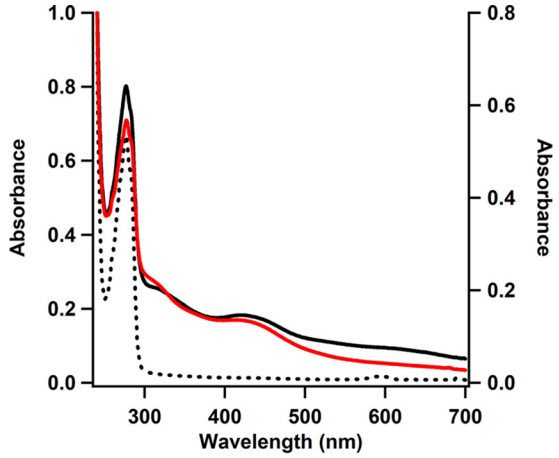

Figure 3. *E. coli* NfuA C-terminal domain, but not the N-terminal domain, coordinates a [4Fe–4S] cluster. UV-visible spectrum of 30 μM as-isolated *E. coli* NfuA N-terminal domain (*black dotted trace*), 30 μM as-isolated *E. coli* NfuA C-terminal domain (*black solid trace*), and full-length *E. coli* NfuA (*solid red trace*).

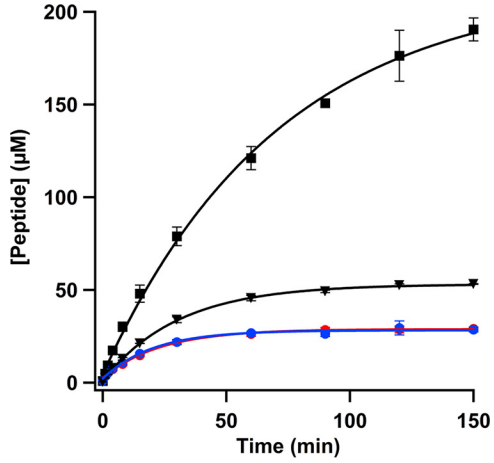

Figure 4. Effect of NfuA truncations on LipA activity. Effect of *E. coli* NfuA N-terminal domain and C-terminal domain on LipA activity. LipA only control (*closed red circles*), LipA + NfuA N-terminal domain (*closed blue circles*), LipA + WT NfuA control (*closed black squares*), LipA + NfuA C-terminal domain (*closed black triangles*). For both panels, reactions included 25 μM LipA, 400 μM NfuA or NfuA domain, 400 μM peptide substrate, 1 mM SAM, and 0.5 μM SAH nucleosidase. Reactions were conducted at room temperature and were initiated by the addition of 2 mM dithionite before quenching with a final concentration of 100 mM H_2SO_4 at various times. *Error bars* represent the mean ± S.D. of three replicates.

to the masses of LipA and NfuA are observed (Fig. 5*B* and Fig. S6). Therefore, although the C-terminal domain of NfuA is essential for the protein's activity, it is dispensable for the interaction between NfuA and LipA.

E. coli NfuA C-terminal domain coordinates a [4Fe–4S] cluster but does not bind tightly to E. coli LipA

A wealth of evidence has supported a role for [4Fe–4S] cluster coordination at a dimer interface by two conserved cysteinyl residues in the Nfu-like C-terminal domain of NfuA (15, 16). We therefore explored whether the C-terminal domain could still coordinate its cluster in the absence of the N-terminal domain. We first overproduced, isolated, and characterized a truncated version of *E. coli* NfuA lacking the N-terminal domain (residues 98–191). Similar to the N-terminal domain, the Nfu-like C-terminal domain was also shown to have a far-UV CD spectrum identical to that of the full-length NfuA protein (18). The C-terminal domain was stable and was overproduced in high yields for analysis. The UV-visible spectrum of the as-isolated protein reveals features of a [4Fe–4S] cluster that are nearly identical to those of the full-length WT protein (Fig. 3). We then tested the effect of the C-terminal domain on LipA's activity. Surprisingly, although the C-terminal domain coordinates a [4Fe–4S] cluster, its ability to restore LipA's auxiliary cluster in a catalytic fashion is largely diminished (Fig. 4, *closed triangles*). Interestingly, however, the NfuA C-terminal domain allows for one additional turnover, albeit at a rate that is six to nine times slower than that in the presence of full-length NfuA (compare Fig. 4, *closed triangles* and *closed squares*). This additional turnover may result from complete destruction of the auxiliary [4Fe–4S] cluster on LipA after one turnover, and the subsequent relatively slow reconstitution of a new [4Fe–4S] cluster during catalysis at the expense of the NfuA C-terminal domain [4Fe–4S] cluster.

Given that the N-terminal domain of NfuA is found to interact with LipA in the absence of the NfuA C-terminal domain, we hypothesized that the C-terminal domain alone may be unable to recognize LipA or does so poorly. Therefore, a similar interaction analysis by molecular-sieve chromatography was conducted to assess whether LipA and the NfuA C-terminal domain interact tightly (Fig. 5*C*). LipA alone (*dotted trace*) elutes at 61.1 ml, corresponding to an experimental mass of 45.2 kDa (theoretical mass is 38.2 kDa). The C-terminal domain of NfuA alone elutes at 77.0 ml (*dashed trace*), corresponding to an experimental mass of 11.8 kDa (theoretical mass is 12.8 kDa). The sample containing an equimolar mixture of LipA and the NfuA C-terminal domain (*solid trace*) contains two major peaks: one peak at 60.9 ml and another at 77.0 ml. The first peak corresponds to LipA alone, whereas the second peak corresponds to the NfuA C-terminal domain. The absence of a shift in the elution volumes suggests that the two proteins do not form a tight complex as was observed previously for the full-length NfuA and LipA (17), and for the NfuA N-terminal domain and LipA, as demonstrated in this work. Fractions corresponding to the major peak were analyzed by SDS-PAGE, confirming that the two proteins do not co-elute (Fig. 5*D*). The inability to interact tightly with LipA may explain the observation that the C-terminal domain alone has a limited effect on LipA's activity, despite the observation that it coordinates a [4Fe–4S] cluster. Together, our analysis suggests that the NfuA N-terminal domain is essential for recognizing LipA and interacting with it, and that in its absence, NfuA is unable to regenerate LipA's auxiliary cluster in a catalytic fashion.

NfuA from Mycobacterium tuberculosis also activates E. coli LipA

Given the structural studies that have been carried out on LipA from *Mycobacterium tuberculosis* (*Mt*) (10), we assessed whether *Mt* NfuA can also regenerate *E. coli* LipA's auxiliary Fe–S cluster. Inspection of an alignment of the two protein sequences shows that the primary structure of *Mt* NfuA shares 89% amino acid identity with the primary structure of *E. coli* NfuA, containing two domains corresponding to the N-termi-

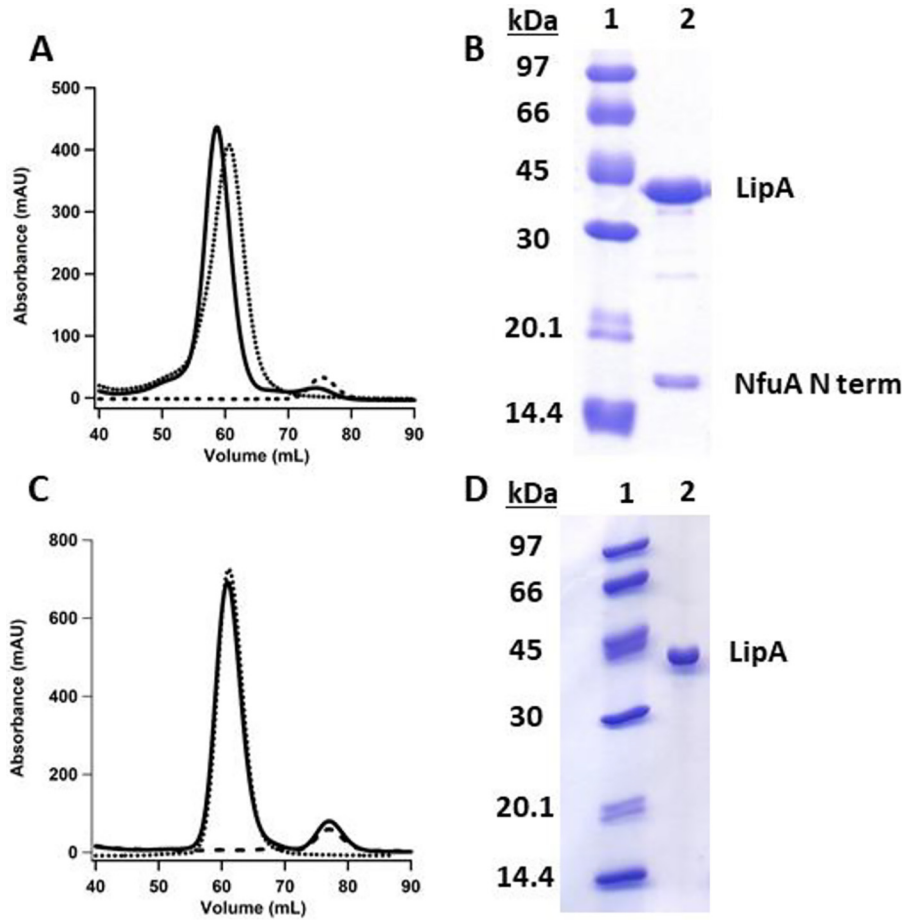

Figure 5. N-terminal domain of *E. coli* NfuA alone interacts with *E. coli* LipA. *A*, a control sample containing 100 μM LipA (*dotted trace*) eluted at 60.6 ml with an experimental calculated size of 44.3 kDa (theoretical size 38.2 kDa). A second control sample containing 100 μM NfuA N-terminal domain (*dashed trace*) eluted at 75.3 ml, with an experimental calculated size of 12.5 kDa (theoretical size 12.6 kDa). A sample containing LipA + the NfuA N-terminal domain (*solid trace*) eluted at 58.6 ml, corresponding to a calculated size of 52.4 kDa (theoretical size of complex 50.8 kDa). *B*, SDS-PAGE analysis of the LipA + NfuA N-terminal domain fractions, confirming the presence of both proteins. *Lane 1*: Molecular weight ladder; *lane 2*: LipA + NfuA N-terminal domain fractions. *C*, a control sample containing 100 μM LipA (*dotted trace*) eluted at 61.1 ml, with an experimental calculated size of 45.2 kDa (theoretical size 38.2 kDa). A second control sample containing 100 μM NfuA C-terminal domain (*dashed trace*) eluted at 77.0 ml, with an experimental calculated size of 11.8 kDa (theoretical size 12.8 kDa). The sample containing LipA + the NfuA C-terminal domain (*solid trace*) contained two peaks eluting at 60.9 ml and 77.0 ml, corresponding to calculated sizes of 47.3 kDa and 12.3 kDa, respectively (theoretical size of complex 51.0 kDa). *D*, SDS-PAGE analysis of the LipA + NfuA C-terminal domain fractions, confirming the absence of the NfuA C-terminal domain in fractions containing LipA. *Lane 1*: Molecular weight ladder; *lane 2*: LipA fraction.

nal A-type domain and the C-terminal Nfu-like domain (Fig. S4). The UV-visible spectrum of as-isolated *Mt* NfuA contains features that are consistent with those of a [4Fe–4S] cluster (Fig. S3). Further, when *Mt* NfuA is included in LipA activity assays, product formation is nearly identical to that in reactions containing *E. coli* NfuA (Fig. 6). In this experiment, 20 μM LipA catalyzes formation of 10 μM lipoyl product after 2.5 h in the absence of NfuA. In the presence of *E. coli* NfuA (*closed squares*) or *Mt* NfuA (*closed triangles*), 20 μM *E. coli* LipA catalyzes formation of ~100 μM lipoyl product in each case. These results suggest that NfuA from other organisms with a similar domain architecture as that of *E. coli* NfuA can fulfill a similar role in LipA catalysis.

LipA turnover is not enhanced by NfuA when using a peptide substrate containing an 8-thiooctanoyllysyl moiety

Early studies of lipoic acid biosynthesis showed that 8-thiooctanoic acid is converted into lipoic acid when administered to growing *E. coli*, but not as well as when octanoic acid is administered (21–23). Fig. 7 shows lipoyl product formation when a peptide substrate containing an 8-thiooctanoyllysyl amino acid residue is acted upon by LipA in the presence of 400 μM NfuA. As can be observed, the lipoyl product levels off at a concentration that is nearly stoichiometric with that of LipA (75 μM) in the reaction (*closed circles*). By contrast, when a peptide substrate containing an octanoyllysyl amino acid is used (*closed squares*), additional turnovers take place. Our model predicts that in the absence of chemistry that results in sulfur insertion at C8, the 8-thiooctanoyl substrate is converted to a lipoyl product that is still bonded to the auxiliary Fe–S cluster. This appendage, and/or the lack of partial or full destruction of the auxiliary cluster, is expected to inhibit cluster transfer from NfuA to LipA.

The addition of an A-type domain to S. aureus Nfu supports multiple turnover by LipA

The observation that the *E. coli* NfuA N-terminal domain is required to regenerate *E. coli* LipA led us to ask whether other Nfu-type proteins that lacked this domain could restore *E. coli* LipA's auxiliary cluster during catalysis. To address this ques-

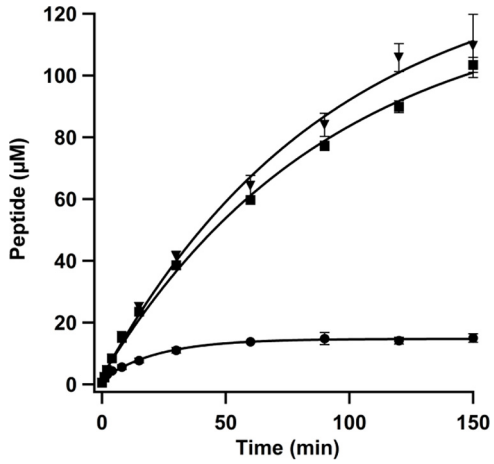

Figure 6. NfuA from *Mycobacterium tuberculosis* also activates *E. coli* LipA. Effect of *Mt* NfuA on LipA activity. LipA only control (*closed circles*). LipA + *E. coli* NfuA control (*closed squares*). LipA + *Mt* NfuA (*closed triangles*). Reactions included 20 μM LipA, 400 μM *E. coli* NfuA or *Mt* NfuA, 400 μM peptide substrate, 700 μM SAM, and 0.5 μM SAH nucleosidase. Reactions were conducted at room temperature and were initiated by the addition of dithionite to a final concentration of 2 mM. At designated times, samples were removed and the reaction was quenched by addition of H_2SO_4 to a final concentration of 100 mM. *Error bars* represent the mean ± S.D. of three replicates.

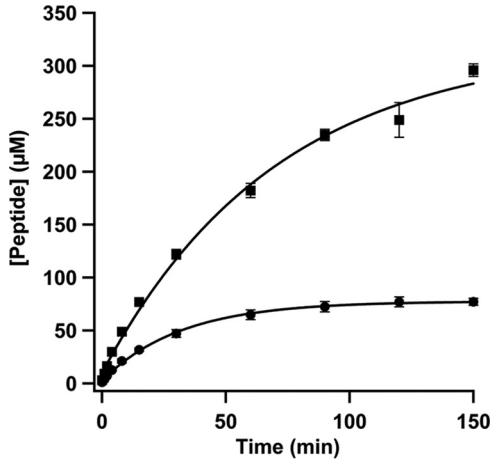

Figure 7. Effect of an 8-thiooctanoyllysyl peptide substrate on catalysis. The reaction (*closed circles*) contained 75 μM LipA, 400 μM NfuA, 400 μM 8-thiooctanoyllysyl peptide substrate, 700 μM SAM, and 0.5 μM SAH nucleosidase. A control reaction using the normal peptide substrate (400 μM) under the same reaction conditions is also shown (*closed squares*). Reactions were conducted at room temperature and were initiated by the addition of dithionite to a final concentration of 2 mM. At designated times, samples were removed and the reaction was quenched by addition of H_2SO_4 to a final concentration of 100 mM. *Error bars* represent the mean ± S.D. of three replicates.

tion, we initially overproduced and isolated Nfu from *S. aureus* and used it in LipA reactions. The sequence homology between *E. coli* NfuA and *S. aureus* Nfu is limited to the C-terminal domain (Fig. S4). The UV-visible spectrum of *S. aureus* Nfu in its as-isolated state contains features that support the presence of a [4Fe–4S] cluster (Fig. S5), consistent with what was reported previously (24). However, when *S. aureus* Nfu is included in activity assays, its effect on LipA's activity is minimal, as shown in Fig. 8. In the presence of 400 μM *S. aureus* NfuA, 25 μM LipA catalyzes formation of ~25 μM product (Fig. 8, *closed triangles*), whereas in its absence, it catalyzes formation of ~15 μM product (Fig. 8, *closed circles*).

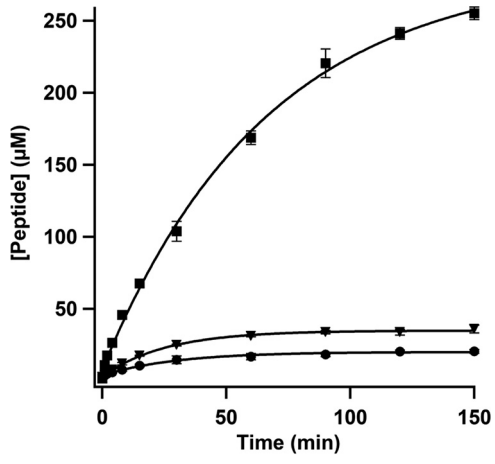

Figure 8. Effect of *S. aureus* Nfu and *E. coli* NfuA N-terminal domain–*S. aureus* Nfu fusion protein on *E. coli* LipA activity. LipA only control (*closed circles*). LipA + *S. aureus* Nfu (*closed triangles*). LipA + *E. coli* NfuA N-terminal domain–*S. aureus* Nfu fusion protein (*closed squares*). Reactions included 25 μM LipA, 400 μM peptide substrate, 1 mM SAM, and 0.5 μM SAH nucleosidase. When appropriate 400 μM *S. aureus* Nfu or 400 μM *E. coli* NfuA N-terminal domain–*S. aureus* Nfu fusion protein were included. Reactions were conducted at room temperature and were initiated by the addition of dithionite to a final concentration of 2 mM. At designated times, samples were removed and the reaction was quenched by addition of H_2SO_4 to a final concentration of 100 mM. *Error bars* represent the mean ± S.D. of three replicates.

The effect of *S. aureus* Nfu on the LipA reaction is similar to that of the C-terminal domain of *E. coli* NfuA. The A-type domain in *E. coli* NfuA, which is shown to be essential in this work, is absent in *S. aureus* Nfu. We therefore created a fusion protein consisting of the *E. coli* NfuA N-terminal domain (residues 1–117) attached to *S. aureus* Nfu. Upon addition of the *E. coli* NfuA N-terminal domain *S. aureus* Nfu fusion to an *E. coli* LipA reaction, significant enhancement of lipoyl product formation is observed, providing more evidence for the essential role of this domain. Now, 25 μM LipA catalyzes formation of greater than 250 μM lipoyl product in 2.5 h (Fig. 8, *closed squares*).

Discussion

The recent demonstration that *E. coli* NfuA engenders multiple turnovers by *E. coli* LipA by restoring its Fe–S cluster cofactor provided the groundwork for expanding our understanding of this complex system. In this work, we confirm the critical role of the cysteinyl residues in the C-terminal domain of *E. coli* NfuA as coordinating ligands to an Fe–S cluster that is housed at the interface between two NfuA monomers, and show that the cysteinyl residues in the N-terminal domain have no apparent effect on cluster coordination or cluster transfer to LipA. In addition, we provide a detailed investigation of the essential role of the *E. coli* NfuA N-terminal domain in interacting with *E. coli* LipA, which was previously proposed to aid in protein–protein interactions (18). The C-terminal domain, which is homologous to many Nfu proteins, is fully capable of coordinating its cluster in the absence of the N-terminal domain, yet is unable to allow LipA to become catalytic, likely because it lacks the domain responsible for recognizing and interacting with *E. coli* LipA. *Mt* NfuA, which is highly homologous to the *E. coli* NfuA, is another NfuA that also contains the A-type domain, and engenders an identical effect on *E. coli* LipA. Interestingly, Nfu from *S. aureus*, which lacks the N-ter-

minal A-type domain, does not affect the activity of *E. coli* LipA, whereas a genetic fusion that adds the *E. coli* NfuA N-terminal domain to the *S. aureus* Nfu protein engenders catalytic activity by *E. coli* LipA. It is tempting to consider the possibility that the domain architecture of *E. coli* NfuA is organized to contain two components with separate essential functions.

Cumulatively, our results highlight the role of the so-called degenerate A-type N-terminal domain as having an essential function. Although our results provide further insight into the regeneration of *E. coli* LipA's auxiliary cluster, significant gaps still remain in our understanding of the cluster restoration by NfuA. Our initial evidence that *E. coli* LipA can use an 8-thiooctanoyllysyl-containing peptide as a substrate, but not in a catalytic fashion, suggests that its cluster must be significantly (a [2Fe–2S] cluster or smaller) degraded before NfuA intervenes. Studies to provide a more detailed mechanism of the state of the cluster on NfuA as it is being transferred to LipA are currently underway.

Experimental procedures

General methods and instruments

The PCR was conducted using a Bio-Rad S1000 thermocycler. DNA sequencing was performed at the Penn State Genomics Core Facility. Amino acid analysis was performed at the UC Davis Proteomics Core Facility. UV-visible spectra were recorded on a Cary 50 spectrophotometer from Varian (Walnut Creek, CA) with the associated WinUV software package. All anaerobic experiments were conducted in a Coy Anaerobic Chamber (Grass Lake, MI). High-performance liquid chromatography (HPLC) with detection by MS (LC-MS) was conducted using an Agilent Technologies (Santa Clara, CA) 1200 system coupled to an Agilent Technologies 6410 QQQ mass spectrometer. Data collection and analysis were performed using the associated MassHunter software. Analytical molecular-sieve chromatography was performed on an ÄKTA system (GE Healthcare) housed in a Coy Anaerobic Chamber equipped with a HiPrep 16/60 Sephacryl S-200 HR column (GE Healthcare). SDS-PAGE was performed using a mini vertical electrophoresis unit from Hoefer (Holliston, MA).

Cloning of genes encoding E. coli LipA; E. coli NfuA; and E. coli NfuA C39A, C44A, C149A, and C152A variants into pET28a

The construction of the *E. coli lipA*-pET28a and *E. coli nfuA*-pET28a expression vectors has been described previously (5, 17). *E. coli nfuA*-pET28a C39A, C44A, C149A, and C152A variants were constructed by site-directed mutagenesis using the Stratagene QuikChange II kit (Agilent Technologies) along with primers listed in Table S1. However, *Pfu* polymerase was substituted with Vent polymerase in the polymerase chain reaction. *E. coli nfuA*-pET28a plasmid DNA was used as the DNA template, and DNA sequencing was used to confirm the desired substitutions.

Cloning of genes corresponding to E. coli NfuA N-terminal and C-terminal domains into pET28a

The gene fragments corresponding to *E. coli* NfuA N-terminal domain (amino acid residues 1–97) and C-terminal domain (amino acid residues 98–191) were PCR-amplified using the *E. coli nfuA*-pET28a plasmid as a DNA template. The primers used for amplification of the N-terminal domain and C-terminal domain introduced an NdeI restriction site at the 5′ end of the gene and a XhoI restriction site at the 3′ end. The gene fragments were digested and ligated into a pET28a vector digested with the same enzymes. Primers used for the constructs can be found in Table S1.

Cloning of the Mycobacterium tuberculosis nfuA gene

The gene encoding NfuA from *Mycobacterium tuberculosis* was codon-optimized for expression in *E. coli* by GeneArt Gene Synthesis (Thermo Fisher Scientific) and was received as a construct in plasmid pMA-T. The gene contained an NdeI restriction site at the 5′ end and an XhoI restriction site at the 3′ end. The gene was digested with these two enzymes and then ligated into a pET28a vector that was similarly digested. The desired construct was confirmed by DNA sequencing.

Cloning of S. aureus Nfu and S. aureus Nfu–E. coli NfuA N-terminal domain fusion protein into pET28a

Genes encoding Nfu (SAUSA300_0839) from *S. aureus* and a genetic fusion consisting of the N-terminal domain of *E. coli* NfuA (amino acids 1–117) attached to *S. aureus* Nfu were codon-optimized for expression in *E. coli* and received as constructs in plasmid pMA-T from GeneArt Gene Synthesis (Thermo Fisher Scientific). Both genes contained an NdeI restriction site at the 5′ end and an XhoI restriction site at the 3′ end. They were each digested with NdeI and XhoI and then ligated into pET28a that was similarly digested. The desired constructs were confirmed by DNA sequencing.

Overproduction of WT E. coli NfuA and NfuA variants, as well as Mt NfuA, S. aureus Nfu, and the E. coli NfuA N-terminal domain–S. aureus Nfu fusion protein

The overproduction of full-length *E. coli* NfuA has been previously described (17). *E. coli* NfuA C39A, C44A, C149A, C152A, NfuA N-terminal domain, NfuA C-terminal domain, *Mt* NfuA, *S. aureus* Nfu, and the *E. coli* NfuA N-terminal domain–*S. aureus* Nfu fusion were overproduced exactly as described for the full-length *E. coli* NfuA. Briefly, BL21(DE3) cells were co-transformed with the construct encoding the desired gene and plasmid pDB1282, which encodes the genes in the *isc* operon from *Azotobacter vinelandii* (25, 26). A single colony was used to inoculate 200 ml lysogeny broth supplemented with 50 μg/ml kanamycin and 100 μg/ml ampicillin, and the starter culture was incubated overnight at 37 °C with shaking at 250 rpm. The following day, 20 ml of the starter culture was used to inoculate four 6-liter flasks containing 4 liters M9 minimal media supplemented with 50 μg/ml kanamycin and 100 μg/ml ampicillin. The *E. coli* strains were cultured at 37 °C with shaking at 180 rpm. At an A_{600} = 0.3, 0.2% arabinose was added to induce expression of the genes encoded in the pDB1282 plasmid. At an A_{600} = 0.6, 50 μM $FeCl_3$ was added to the cultures, and the flasks were placed in an ice-water bath for ~30 min. Once chilled, expression of the desired gene was induced by the addition of 200 μM isopropyl 1-thio-β-D-galactopyranoside (final concentration) and allowed to proceed for ~18 h at 18 °C with shaking at 180 rpm. Bacterial cells were

harvested by centrifugation at 7500 × *g* for 12 min. The resulting cellular pellet was flash-frozen in liquid N_2 and stored in liquid N_2 until further use.

Isolation of E. coli NfuA and NfuA variants, as well as Mt NfuA, S. aureus Nfu, and the E. coli NfuA N-terminal domain–S. aureus Nfu fusion protein

The purification of *E. coli* WT NfuA has been described previously (17). NfuA C39A, C44A, C139A, C152A, NfuA N-terminal domain, NfuA C-terminal domain, *Mt* NfuA, *S. aureus* Nfu, and the *E. coli* NfuA N-terminal domain–*S. aureus* Nfu fusion protein were purified exactly as described for WT *E. coli* NfuA. All purification steps were carried out in an anaerobic chamber containing <1 ppm O_2 (Coy Laboratory Products, Grass Lake, MI), with the exception of the centrifugation steps. In these instances, solutions were loaded into bottles that were then tightly sealed before being removed from the chamber for centrifugation. The cell pellet was resuspended in Buffer A (50 mM HEPES, pH 7.5, 300 mM KCl, 20 mM imidazole, and 10 mM β-mercaptoethanol). Lysozyme (1 mg/ml) and DNase I (0.1 mg/ml) were added, and the solution was stirred at room temperature for 30 min. The cells were lysed by sonic disruption, and the lysate was centrifuged at 45,000 × *g* for 1 h. The supernatant was applied to a nickel-nitrilotriacetic acid (Ni-NTA) resin (Qiagen) column pre-equilibrated in Buffer A. The column was washed with Buffer B (50 mM HEPES, pH 7.5, 300 mM KCl, 45 mM imidazole, 10 mM β-mercaptoethanol, and 10% glycerol), and the protein was eluted using Buffer C (50 mM HEPES, pH 7.5, 300 mM KCl, 500 mM imidazole, 10 mM β-mercaptoethanol, and 10% glycerol). The protein was concentrated to 2.5 ml and then exchanged into Storage Buffer (50 mM HEPES, pH 7.5, 300 mM KCl, 1 mM DTT, 15% glycerol) using a PD-10 column (GE Healthcare). The protein was aliquoted, flash-frozen in liquid N_2, and stored in liquid N_2 until further use. The *E. coli* NfuA N-terminal domain was further purified by size-exclusion chromatography using a HiPrep 16/60 Sephacryl S-200 HR column (GE Healthcare) connected to an ÄKTA FPLC system housed within an anaerobic chamber. The column was equilibrated in Storage Buffer at a constant flow rate of 0.5 ml/min before application and subsequent elution of the protein at the same flow rate. The purity of the isolated proteins was analyzed by SDS-PAGE (12.5% gel) and determined to be >95%. The protein concentration was determined via the Bradford method (27). Amino acid analysis revealed that the Bradford method overestimates the protein concentration of *E. coli* NfuA by a factor of 1.18, *Mt* NfuA by a factor of 1.03, *S. aureus* Nfu by a factor of 1.26, and the *E. coli* C-terminal domain by a factor of 1.24 (UC Davis Proteomics Core). Colorimetric iron and sulfide analyses were used to estimate the iron and sulfide content per polypeptide (28, 29).

Overproduction and isolation of E. coli LipA

The overproduction and isolation of *E. coli* LipA has been described previously (5). This method was performed exactly as described with the following amendment. In the overproduction of *E. coli* LipA, the M9 minimal media was inoculated with 0.2 ml of starter culture, which was allowed to grow overnight at 37 °C with shaking at 180 rpm. The following day, expression of genes on pDB1282 was induced by addition of arabinose (0.2% final concentration) at A_{600} = 0.3. At an A_{600} = 0.6, 50 μM $FeCl_3$ was added to the cultures, and the flasks were placed in an ice-water bath for ~30 min. Once chilled, expression of the *lipA* gene was induced by the addition of isopropyl 1-thio-β-D-galactopyranoside (200 μM final concentration) and allowed to proceed for ~18 h at 18 °C with shaking at 180 rpm. Bacterial cells were harvested by centrifugation at 7500 × *g* for 12 min. The resulting cell pellet was flash-frozen in liquid N_2 and stored in liquid N_2 until further use. *E. coli* LipA was isolated using methods described previously with no modifications (5).

Analytical molecular-sieve chromatography

Physical interactions between *E. coli* LipA and truncated versions of *E. coli* NfuA, as well as among *E. coli* ErpA, *E. coli* NfuA, and *E. coli* LipA, were probed by analytical molecular-sieve chromatography. A 500 μl mixture of standards composed of cytochrome *c*, carbonic anhydrase, bovine serum album, alcohol dehydrogenase, β-amylase, and blue dextran was applied to a HiPrep 16/60 Sephacryl S-200 HR column (GE Healthcare) connected to an ÄKTA FPLC system housed within an anaerobic chamber (<1 ppm O_2). The column was equilibrated in 50 mM HEPES, pH 7.5, 300 mM KCl, 15% glycerol, and 5 mM DTT (freshly prepared immediately before use) at a constant flow rate of 0.5 ml/min before applying and eluting protein samples. The log molecular weight of each standard was plotted against its elution volume after correcting for the void volume of the column. The linear equation was then used to estimate the molecular weight of each sample. The chromatogram of the standards as well as the standard curve used for experimental calculations are shown in Fig. S2. The samples included the following in a total 500 μl volume: 100 μM LipA only, 100 μM full-length NfuA only, 100 μM NfuA N-terminal domain only, 100 μM NfuA C-terminal domain only, a mixture of 100 μM LipA and 100 μM NfuA N-terminal domain, and a mixture of 100 μM LipA and 100 μM NfuA C-terminal domain. The interaction was determined by the presence of a shift in the elution volume of samples as well as by the calculated experimental weights for each of the peaks. Fractions corresponding to each peak were subjected to SDS-PAGE to determine the presence of each protein.

LC-MS activity determinations

The experimental setup and assay conditions were described in detail in previous publications with a few notable amendments (8, 26). The reactions were conducted under strictly anaerobic conditions in a Coy anaerobic glovebox. Reactions of NfuA variants C39A, C44A, C149A, and C152A (Fig. 2) contained 25 μM LipA, 400 μM NfuA variant or WT protein, 600 μM peptide substrate (Glu-Ser-Val-(N^6-octanoyl)Lys-Ala-Ala-Ser-Asp), 0.5 μM S-adenosylhomocysteine (SAH) nucleosidase, and 1 mM SAM. Reactions testing LipA activity in the presence of NfuA truncations (Fig. 4) included 25 μM LipA, 400 μM WT NfuA or NfuA domain, 400 μM peptide substrate, 1 mM SAM, and 0.5 μM SAH nucleosidase. Reactions comparing the effects of *E. coli* NfuA and *Mt* NfuA (Fig. 6) contained 20 μM LipA, 400 μM *E. coli* NfuA or *Mt* NfuA, 400 μM peptide substrate, 700 μM SAM, and 0.5 μM SAH nucleosidase. The reaction using the 8-thiooctanoyl peptide substrate analog (Fig. 7) included 75 μM

LipA, 400 μM NfuA, 400 μM peptide substrate (control) or 8-thiooctanoyl–containing peptide substrate, 0.5 μM SAH nucleosidase, and 1 mM SAM. Reactions testing the effect of *S. aureus* Nfu or the *E. coli* NfuA N-terminal domain–*S. aureus* Nfu fusion protein (Fig. 8) contained 25 μM LipA, 400 μM *S. aureus* Nfu or fusion protein, 400 μM peptide substrate, 0.5 μM SAH nucleosidase, and 1 mM SAM. Reactions were conducted at room temperature and were initiated by addition of sodium dithionite to a final concentration of 2 mM. The reactions were quenched at appropriate times with H_2SO_4 at a final concentration of 100 mM. All reactions were performed in triplicate. Detection of substrates and products was performed using electrospray ionization MS in positive mode (ESI^+-MS) with the following parameters: A nitrogen gas temperature of 340 °C and flow rate of 9.0 liters/min, a nebulizer pressure of 40 psi, and a capillary voltage of 4000 V. Substrates and products were detected using multiple reaction monitoring (Table S2). The reaction mixture was separated on an Agilent Technologies Zorbax Extend-C18 Rapid Resolution HT column (4.6 mm × 50 mm, 1.8 μm particle size) equilibrated in 98% solvent A (0.1% formic acid, pH 2.6) and 2% solvent B (100% acetonitrile). A gradient of 2–23% solvent B was applied from 0.8 min to 3.5 min and maintained at 23% solvent B until 8 min, before returning to solvent B to 2% from 8 to 10 min. A flow rate of 0.4 ml/min was maintained throughout the method. The column was allowed to re-equilibrate for 2 min under the initial conditions between sample injections.

Author contributions—E. L. M. and S. J. B. conceptualization; E. L. M. data curation; E. L. M. and S. J. B. formal analysis; E. L. M. and S. J. B. supervision; E. L. M., A. N. R., and Z. R. D. investigation; E. L. M. methodology; E. L. M. and S. J. B. writing-original draft; E. L. M. and S. J. B. project administration; E. L. M. and S. J. B. writing-review and editing; S. J. B. resources; S. J. B. funding acquisition; S. J. B. validation.

References

1. Broderick, J. B., Duffus, B. R., Duschene, K. S., and Shepard, E. M. (2014) Radical *S*-adenosylmethionine Enzymes. *Chem. Rev.* **114,** 4229–4317 CrossRef Medline
2. Sofia, H. J., Chen, G., Hetzler, B. G., Reyes-Spindola, J. F., and Miller, N. E. (2001) Radical SAM, a novel protein superfamily linking unresolved steps in familiar biosynthetic pathways with radical mechanisms: Functional characterization using new analysis and information visualization methods. *Nucleic Acids Res.* **29,** 1097–1106 CrossRef Medline
3. Frey, P. A., and Booker, S. J. (2001) Radical mechanisms of *S*-adenosylmethionine-dependent enzymes. in *Advances in Protein Chemistry*, Vol. 58, pp. 1–45, Elsevier, Amsterdam, The Netherlands CrossRef
4. Lanz, N. D., and Booker, S. J. (2015) Auxiliary iron-sulfur cofactors in radical SAM enzymes. *Biochim. Biophys. Acta* **1853,** 1316–1334 CrossRef Medline
5. Cicchillo, R. M., Iwig, D. F., Jones, A. D., Nesbitt, N. M., Baleanu-Gogonea, C., Souder, M. G., Tu, L., and Booker, S. J. (2004) Lipoyl synthase requires two equivalents of *S*-adenosyl L-methionine to synthesize one equivalent of lipoic acid. *Biochemistry* **43,** 6378–6386 CrossRef Medline
6. Cicchillo, R. M., Lee, K. H., Baleanu-Gogonea, C., Nesbitt, N. M., Krebs, C., and Booker, S. J. (2004) *Escherichia coli* lipoyl synthase binds two distinct [4Fe–4S] clusters per polypeptide. *Biochemistry* **43,** 11770–11781 CrossRef Medline
7. Douglas, P., Kriek, M., Bryant, P., and Roach, P. L. (2006) Lipoyl synthase inserts sulfur atoms into an octanoyl substrate in a stepwise manner. *Angew. Chem. Int. Ed. Engl.* **45,** 5197–5199 CrossRef Medline
8. Lanz, N. D., Pandelia, M. E., Kakar, E. S., Lee, K. H., Krebs, C., and Booker, S. J. (2014) Evidence for a catalytically and kinetically competent enzyme-substrate cross-linked intermediate in catalysis by lipoyl synthase. *Biochemistry* **53,** 4557–4572 CrossRef Medline
9. Lanz, N. D., Rectenwald, J. M., Wang, B., Kakar, E. S., Laremore, T. N., Booker, S. J., and Silakov, A. (2015) Characterization of a radical intermediate in lipoyl cofactor biosynthesis. *J. Am. Chem. Soc.* **137,** 13216–13219 CrossRef Medline
10. McLaughlin, M. I., Lanz, N. D., Goldman, P. J., Lee, K. H., Booker, S. J., and Drennan, C. L. (2016) Crystallographic snapshots of sulfur insertion by lipoyl synthase. *Proc. Natl. Acad. Sci. U.S.A.* **113,** 9446–9450 CrossRef Medline
11. Ayala-Castro, C., Saini, A., and Outten, F. W. (2008) Fe–S cluster assembly pathways in bacteria. *Microbiol. Mol. Biol. Rev.* **72,** 110–125, table of contents CrossRef Medline
12. Fontecave, M., and Ollagnier-de-Choudens, S. (2008) Iron-sulfur cluster biosynthesis in bacteria: Mechanisms of cluster assembly and transfer. *Arch. Biochem. Biophys.* **474,** 226–237 CrossRef Medline
13. Johnson, D. C., Dean, D. R., Smith, A. D., and Johnson, M. K. (2005) Structure, function, and formation of biological iron-sulfur clusters. *Annu. Rev. Biochem.* **74,** 247–281 CrossRef Medline
14. Rouault, T. A., and Tong, W. H. (2008) Iron–sulfur cluster biogenesis and human disease. *Trends Genet.* **24,** 398–407 CrossRef Medline
15. Angelini, S., Gerez, C., Ollagnier-de Choudens, S., Sanakis, Y., Fontecave, M., Barras, F., and Py, B. (2008) NfuA, a new factor required for maturing Fe/S proteins in *Escherichia coli* under oxidative stress and iron starvation conditions. *J. Biol. Chem.* **283,** 14084–14091 CrossRef Medline
16. Bandyopadhyay, S., Naik, S. G., O'Carroll, I. P., Huynh, B. H., Dean, D. R., Johnson, M. K., and Dos Santos, P. C. (2008) A proposed role for the *Azotobacter vinelandii* NfuA protein as an intermediate iron-sulfur cluster carrier. *J. Biol. Chem.* **283,** 14092–14099 CrossRef Medline
17. McCarthy, E. L., and Booker, S. J. (2017) Destruction and reformation of an iron-sulfur cluster during catalysis by lipoyl synthase. *Science* **358,** 373–377 CrossRef Medline
18. Py, B., Gerez, C., Angelini, S., Planel, R., Vinella, D., Loiseau, L., Talla, E., Brochier-Armanet, C., Garcia Serres, R., Latour, J. M., Ollagnier-de Choudens, S., Fontecave, M., and Barras, F. (2012) Molecular organization, biochemical function, cellular role and evolution of NfuA, an atypical Fe–S carrier. *Mol. Microbiol.* **86,** 155–171 CrossRef Medline
19. Hurley, J. K., Weber-Main, A. M., Hodges, A. E., Stankovich, M. T., Benning, M. M., Holden, H. M., Cheng, H., Xia, B., Markley, J. L., Genzor, C., Gomez-Moreno, C., Hafezi, R., and Tollin, G. (1997) Iron-sulfur cluster cysteine-to-serine mutants of *Anabaena* [2Fe–2S] ferredoxin exhibit unexpected redox properties and are competent in electron transfer to ferredoxin:$NADP^+$ reductase. *Biochemistry* **36,** 15109–15117 CrossRef Medline
20. Subramanian, S., Duin, E. C., Fawcett, S. E. J., Armstrong, F. A., Meyer, J., and Johnson, M. K. (2015) Spectroscopic and redox studies of valence-delocalized $[Fe_2S_2]^+$ centers in thioredoxin-like ferredoxins. *J. Am. Chem. Soc.* **137,** 4567–4580 CrossRef Medline
21. Hayden, M. A., Huang, I. Y., Iliopoulos, G., Orozco, M., and Ashley, G. W. (1993) Biosynthesis of lipoic acid: Characterization of the lipoic acid auxotrophs *Escherichia coli* W1485-lip2 and JRG33-lip9. *Biochemistry* **32,** 3778–3782 CrossRef Medline
22. Reed, K. E., and Cronan, J. E. (1993) Lipoic acid metabolism in *Escherichia coli*: Sequencing and functional characterization of the lipA and lipB genes. *J. Bacteriol.* **175,** 1325–1336 CrossRef Medline
23. White, R. H. (1980) Biosynthesis of lipoic acid: extent of incorporation of deuterated hydroxy- and thiooctanoic acids into lipoic acid. *J. Am. Chem. Soc.* **102,** 6605–6607 CrossRef
24. Mashruwala, A. A., Pang, Y. Y., Rosario-Cruz, Z., Chahal, H. K., Benson, M. A., Mike, L. A., Skaar, E. P., Torres, V. J., Nauseef, W. M., and Boyd, J. M. (2015) Nfu facilitates the maturation of iron-sulfur proteins and participates in virulence in *Staphylococcus aureus*. *Mol. Microbiol.* **95,** 383–409 CrossRef Medline
25. Lanz, N. D., Grove, T. L., Gogonea, C. B., Lee, K. H., Krebs, C., and Booker, S. J. (2012) RlmN and AtsB as models for the overproduction and characterization of radical SAM proteins. *Methods Enzymol.* **516,** 125–152 CrossRef Medline

26. McCarthy, E. L., and Booker, S. J. (2018) Biochemical approaches for understanding iron-sulfur cluster regeneration in Escherichia coli lipoyl synthase during catalysis. *Methods Enzymol.* **606,** 217–239 CrossRef Medline
27. Bradford, M. M. (1976) A rapid and sensitive method for the quantitation of microgram quantities of protein utilizing the principle of protein-dye binding. *Anal. Biochem.* **72,** 248–254 CrossRef Medline
28. Beinert, H. (1978) Micro methods for the quantitative determination of iron and copper in biological material. *Methods Enzymol.* **54,** 435–445 CrossRef Medline
29. Beinert, H. (1983) Semi-micro methods for analysis of labile sulfide and of labile sulfide plus sulfane sulfur in unusually stable iron-sulfur proteins. *Anal. Biochem.* **131,** 373–378 CrossRef Medline

The A-type domain in *Escherichia coli* NfuA is required for regenerating the auxiliary [4Fe–4S] cluster in *Escherichia coli* lipoyl synthase

Erin L. McCarthy, Ananda N. Rankin, Zerick R. Dill and Squire J. Booker

J. Biol. Chem. 2019, 294:1609-1617.
doi: 10.1074/jbc.RA118.006171 originally published online December 11, 2018

Supporting Information

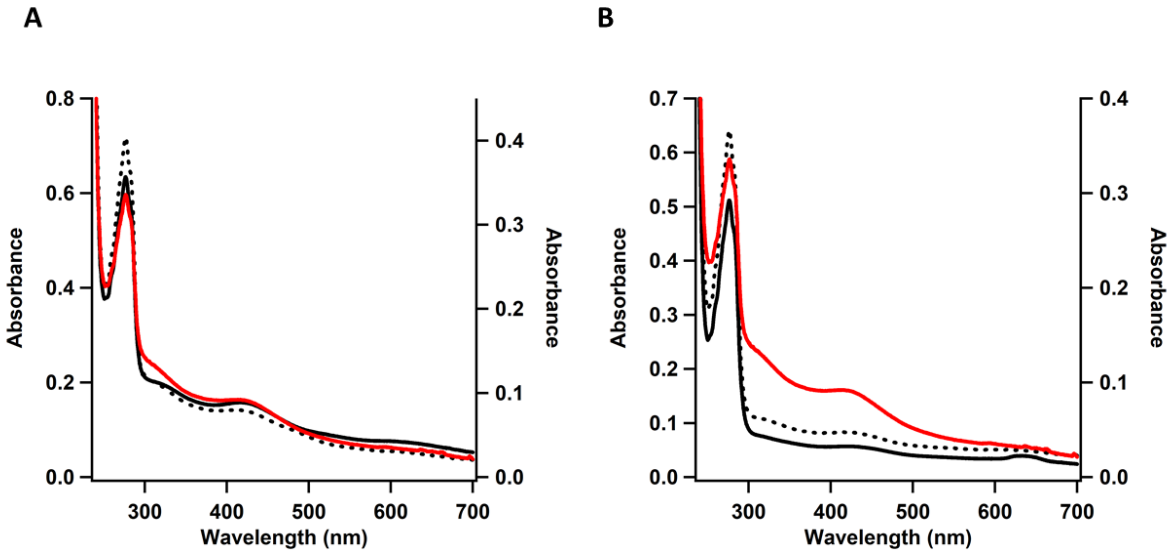

Figure S1. UV-visible Spectra of *E. coli* NfuA C39A, C44A, C149A, and C152A Variants. UV-visible spectrum of (A) 15 µM as-isolated *E. coli* NfuA C39A (black solid trace), C44A (black dotted trace) compared to wild-type NfuA (red solid trace). (B) 15 µM as-isolated *E. coli* NfuA C149A (black solid trace), C152A (black dotted trace), compared to wild-type NfuA reproduced from Figure 3 for comparison (red solid trace).

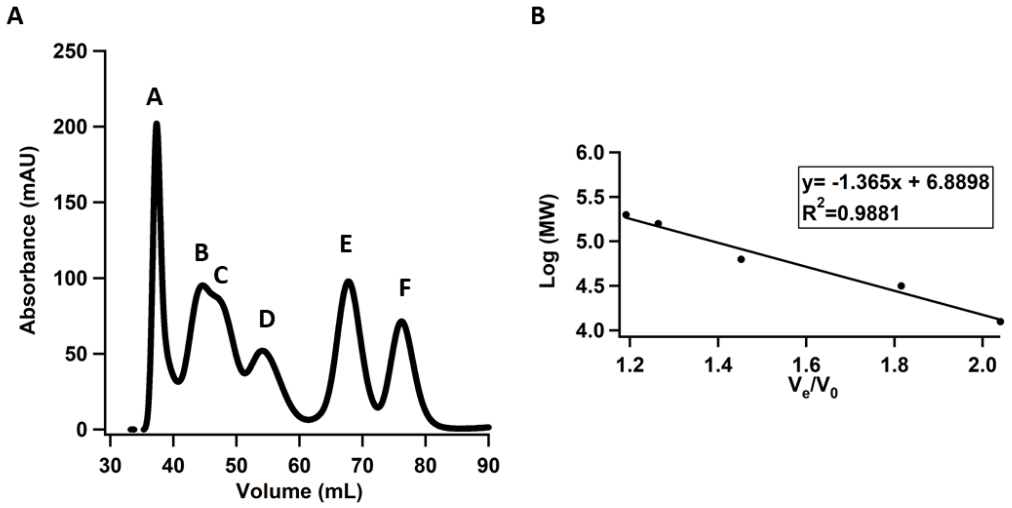

Figure S2. Suite of Standards Used in Analytical Molecular Sieve Chromatography. (A) Chromatogram of the standards used for standard curve generation, monitoring their absorbance at 280 nm: (A) Blue Dextran 2000 kDa, (B) β-Amylase 200 kDa, (C) Alcohol Dehydrogenase 150 kDa, (D) Bovine Serum Albumin 66 kDa, (E) Carbonic Anhydrase 29 kDa, and (F) Cytochrome C, 12.4 kDa. (B) The elution volume of each standard corrected for the void volume of the column was plotted versus the log molecular weight of each of the standards. The linear equation was used to estimate the respective size of each unknown protein based on its elution volume.

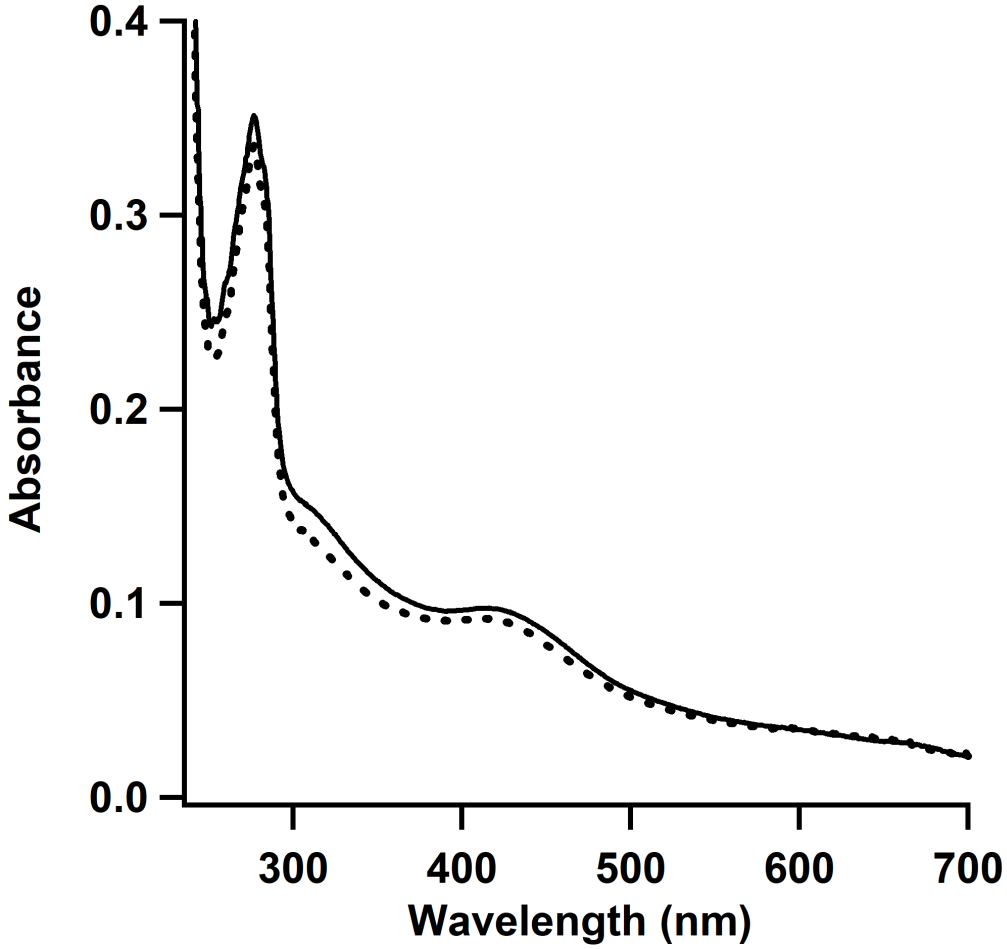

Figure S3. UV-visible Spectrum of *Mt* NfuA. UV-visible spectrum of 15 µM as-isolated NfuA from *Mycobacterium tuberculosis* (solid line) compared to 15 µM as-isolated *E. coli* NfuA reproduced from Figure 3 for comparison (dashed line).

Figure S4. Sequence alignment of NfuA/Nfu from *Escherichia coli (E. coli), Mycobacterium tuberculosis (M. tuberculosis),* and *Staphylococcus aureus (S. aureus).*

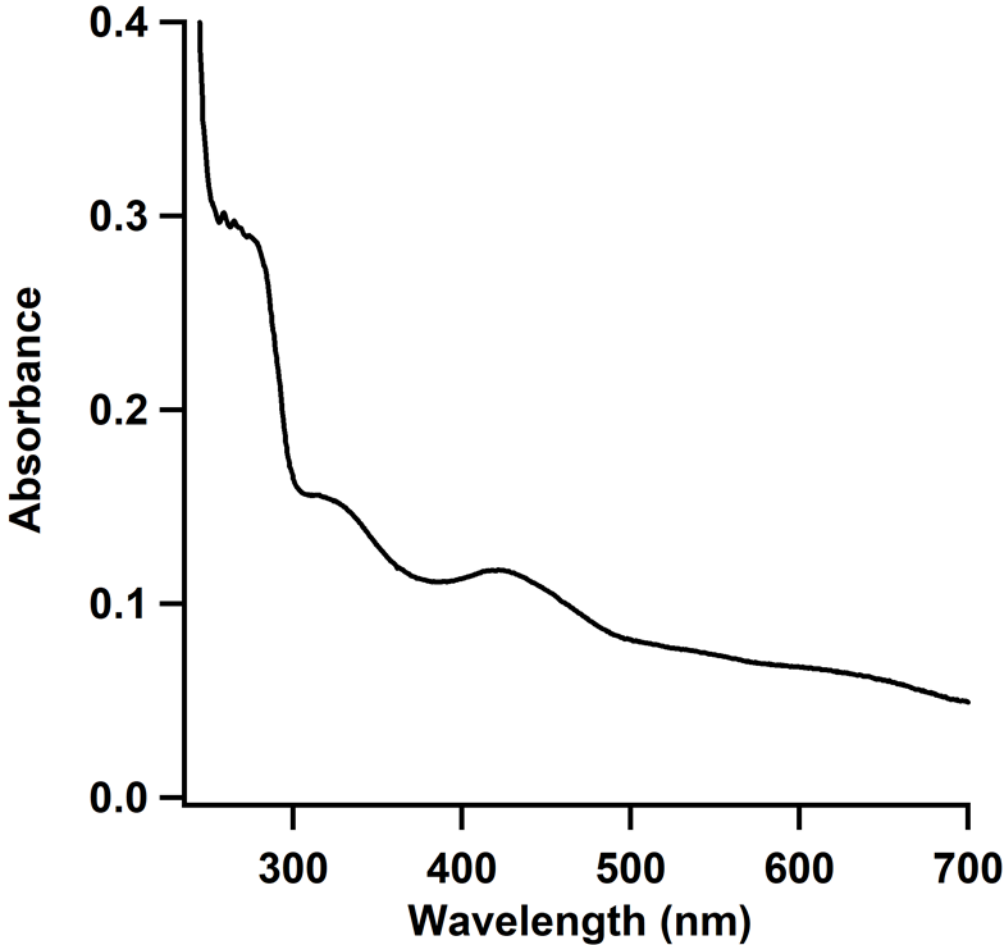

Figure S5. UV-visible spectrum of *S. aureus* Nfu. UV-visible spectrum of 15 μM as-isolated Nfu from *Staphylococcus aureus* (SAUSA300_0839).

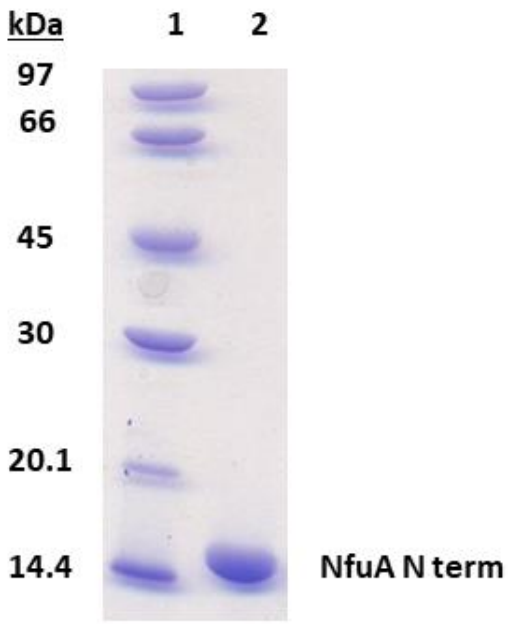

Figure S6. SDS-PAGE of *E. coli* NfuA N terminal Domain. 12.5% SDS-PAGE gel loaded as follows: Lane 1, ladder; Lane 2, NfuA N terminal domain.

Supplementary Table 1. Oligonucleotides used for plasmid construction.

Gene	Vector		Oligonucleotide
nfuA	pET28a	forward	5' CGC GGC GTC AAG CTT ATG ATC CGT ATT TCC GAT GCT GC 3'
		reverse	5' CGC GGC GTC CTC GAG TTA GTA GTA GGA GTG TTC GCC GC 3'
lipA	pET28a	forward	5' GCG GCG TCC ATA TGA GTA AAC CCA TTG TGA TGG AAC GC 3'
		reverse	5′ GCC GGA ATT CTT ACT TAA CTT CCA TCC CTT TCG 3′
nfuA N terminal domain	pET28a	forward	5′ CGC GGC GTC CAT ATG ATC CGT ATT TCC GAT GCT GCA CAA GC 3′
		reverse	5′ CGC GGC GTC CTC GAG TTA TTT GGC GTT CGG GGC TTT CAG CG 3′
nfuA C terminal domain	pET28a	forward	5′ CGC GGC GTC CAT ATG ATG CGT AAA GTG GCA GAC GAT GC 3′
		reverse	5′ CGC GC GTC CTC GAG TTA GTA GTA GGA GTG TTC GCC GC 3′
Cys39Ala	pET28a	forward	5' ACG CCT AAC GCT GAA GCT GGC GTT TCT TAT TGT 3'
		reverse	5' ACA ATA AGA AAC GCC AGC TTC AGC GTT AGG CGT 3'
Cys44Ala	pET28a	forward	5' TGT GGC GTT TCT TAT GCT CCG CCG GAC GCT GTG 3'
		reverse	5' CAC AGC GTC CGG CGG AGC ATA AGA AAC GCC ACA 3'
Cys149Ala	pET28a	forward	5' CAA TTT GGC GGC GGC GCT AAC GGT TGT TCC ATG 3'
		reverse	5' CAT GGA ACA ACC GTT AGC GCC GCC GCC AAA TTG 3'
Cys152Ala	pET28a	forward	5' GGC GGC TGT AAC GGT GCT TCC ATG GTC GAT GTG 3'
		reverse	5' CAC ATC GAC CAT GGA AGC ACC GTT ACA GCC GCC 3'

Supplementary Table 2. Parameters for LC-MS/MS analysis of unlabeled reaction intermediate and product.

Compound	Parent Ion	Fragmentator Voltage	Product Ion 1	Product Ion 2
Octanoyl Peptide	932.5	240	552.3 (37)	210.1 (51)
6-Thio-octanoyl Peptide	964.5	240	584.3 (37)	242.1 (51)
Lipoyl Peptide	996.5	240	616.4 (37)	274.1 (51)
AtsA Peptide (IS)	474.4	135	229.1 (12)	153.1 (26)
Tryptophan (IS)	188.0	130	146.1 (10)	118.0 (21)

*Respective collision energies are in parentheses